ChemComm

Self-assembly of an Organometallic Fe_9O_6 Cluster from Aerobic Oxidation of (tmeda)Fe($CH_2{}^tBu)_2$

Journal:	*ChemComm*
Manuscript ID	CC-COM-01-2020-000011.R1
Article Type:	Communication

COMMUNICATION

Self-assembly of an Organometallic Fe_9O_6 Cluster from Aerobic Oxidation of (tmeda)Fe($CH_2{}^tBu$)$_2$

Received 00th January 20xx,
Accepted 00th January 20xx

DOI: 10.1039/x0xx00000x

Jonathan A. Kephart,[a]† Zachary Hecht,[a]† Brooke N. Livesay,[b] Indrani Bhowmick,[b] Dr. Matthew P. Shores,[b] Dr. V. Codrina Popescu,[c] Dr. Navamoney Arulsamy,[a] Dr. Elliott B. Hulley.*[a]

Aerobic oxidation of (tmeda)Fe($CH_2{}^tBu$)$_2$ in toluene or THF solution leads to the self-assembly of a magic-sized all-ferrous oxide cluster containing the Fe_9O_6 subunit and bearing organometallic and diamine ligands. Mössbauer studies of the cluster are consistent with an all-ferrous assignment and magnetometry reveals complex intracluster and intercluster magnetic interactions.

Molecular clusters are profoundly important species, playing fundamental roles in materials science, nanocatalysis and as models of heterogeneous surfaces and protein active sites.[1] Since aggregation steps are generally unselective and fast, synthetic routes towards large atomic assemblies that result in monodisperse samples are rare. Originally limited to time-controlled hydrothermal methods, recent developments have enabled the syntheses of atomically-precise ligand-stabilized clusters of transition metals and semiconductors,[2,3,12,4–11] wherein conditions are controlled to selectively aggregate monomers and minimize bulk material growth. As a result of these studies of mesoscale entities, the change in physical properties of materials as they progress from the molecular scale to the bulk can be studied in great detail. Since the development of nanoengineered materials (e.g. metal-organic frameworks) depends heavily on the available design elements,[13] modular clusters with a variety of chemical and physical properties are highly desirable.

Metal oxide clusters are of particular interest due to the electrical and magnetic properties of the bulk compounds. Transition metal oxide clusters have nearly always been studied as gas-phase species generated by laser ablation of metals in an oxygen atmosphere.[14–17] Synthetic routes towards chemically isolable atomically-precise clusters of these highly ionic materials are strongly hampered by the tendency for oxides to aggregate in the absence of polydentate ligand frameworks,[18,19] and syntheses are largely limited to hydrothermal conditions that result in carboxylate- or alkoxide-capped clusters and have limited opportunities for further elaboration into nanomaterials.[20–23] Moreover, since syntheses of hybrid MOF-like materials are often also hydrothermal,[13] the incorporation of oxide-based clusters can be complicated by annealing (changing the structure of the oxide subunit) or agglomeration. The present work reports the synthesis and unique magnetic properties of an atomically-precise ferrous oxide cluster that bears highly reactive organometallic ligands, and represents the first synthetic route towards a member of the 'magic-sized' class of metal oxide clusters.[15,16]

While researching unrelated chemistry of first-row transition metal dialkyl compounds, we observed that exposure of organoiron compounds to sub-stoichiometric oxygen led to the formation of a hydrocarbon-soluble complex that crystallized on standing (Figure 1). Treatment of colorless (tmeda)Fe($CH_2{}^tBu$)$_2$ with 0.5 molar equivalents of O_2 (from air) in toluene solution results in the formation of a red-brown solution/suspension. After stirring at room temperature for 4 hours and removal of solvent *in vacuo*, the brown/black residue was extracted with hydrocarbon solvents (e.g. pentane, hexane, heptane, etc.) to yield a brown solution from which deep red crystals of the nine-iron cluster **[Fe_9O_6]**•*solvent* formed (17 % isolated yield based on [Fe] with pentane solvate).

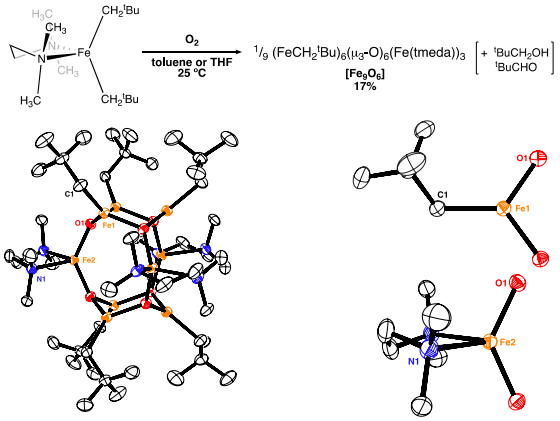

Figure 1. Synthesis (top), solid state structure of **[Fe_9O_6]** (bottom left) and views of the trigonal [(Np)FeO_2] and pseudotetrahedral [(tmeda)FeO_2] (bottom right) subunits. Selected distances and angles: d(Fe1-O1) = 1.907(2) Å, d(Fe1-O1′) = 1.903(2) Å, d(Fe1-C1) = 2.060(3) Å, d(Fe2-O1) = 1.872(2) Å, d(Fe2-N1) = 2.232(2) Å, d(Fe1-Fe1′) = 3.052(1) Å, d(Fe1-Fe2) = 3.249(1) Å, ∠(O1-Fe1-O1′) = 110.08(9)º, ∠(O1-Fe2-O1′) = 130.38(9)º.

[a] *Department of Chemistry, University of Wyoming, Laramie, WY 82071, USA*
[b] *Department of Chemistry, Colorado State University, Fort Collins, CO 80523, USA.*
[c] *Department of Chemistry, University of St. Thomas, St. Paul, MN 55105, USA.*
† These authors contributed equally.
Electronic Supplementary Information (ESI) available: Synthetic, spectroscopic, and magnetometry details. See DOI: 10.1039/x0xx00000x

Although the yield is relatively low, it is consistent for reaction scales up to ~ 1g of (tmeda)Fe($CH_2{}^tBu$)$_2$ and is reasonable for a one-pot reaction that does not require ligands of additional complexity. The product is readily separated from the mother liquor by decantation; crystals of **[Fe_9O_6]** are attracted to an external permanent magnet with sufficient strength that this can be used to aid physical separation. NMR spectral analysis of the mother liquor reveals the presence of peaks consistent with neopentanol, pivalaldehyde, and residual (tmeda)Fe($CH_2{}^tBu$)$_2$ which can be re-isolated *via* crystallization (~ 10 – 15% of the starting [Fe]). The relative amounts of oxidized organic products vary considerably from batch to batch and did not seem correlated with yields.

The cluster crystallizes in the chiral rhombohedral space group $R3_2$, resulting in crystallographic D_3 symmetry, and possesses two distinct iron sites in either an axial or equatorial disposition (Figure 1, bottom). The coordination environment of the axial iron sites is best described as trigonal planar (Σ(angles) = 359.93º), whereas the equatorial iron sites are best described as distorted tetrahedral (τ_4 = 0.81).[24] The cluster is highly air- and moisture-sensitive, but is stable for days under ambient conditions in solution (toluene, benzene, THF) and indefinitely stable in the solid state. The cluster crystallizes on both the three-fold and perpendicular two-fold rotation axes of the crystal lattice, such that one sixth of the molecule is the asymmetric unit, and clusters pack such that they are mutually aligned on the z-axis (Figure 2). There are large voids between molecules (~ 50 Å^3) that contain disordered solvent molecules (Figure 2, left); isostructural crystals have been grown that contain C_nH_{2n+2} hydrocarbons (n = 5 – 9) and toluene, suggesting that crystal growth is somewhat insensitive to the nature of the guest.

Redox-active metal centers in cluster compounds, particularly those with covalent bridging ligands (i.e. 'soft' anions), are notoriously challenging to assign to oxidation states.[25,26] In the present case, standard charges on ligands would predict that the average oxidation state of the nine iron atoms would be +2 (i.e. all ferrous). Zero-field Mössbauer spectroscopy at 5.5 K reveals two quadrupole doublets in a 2:1 ratio (labeled δ_1 and δ_2, respectively), as expected for the two distinct iron environments of **[Fe_9O_6]** (Figure 3, top). The major doublet (δ_1 = 0.41(2) mm/s, ΔE_Q = 1.57(2) mm/s), consistent with the trigonal planar environment on the axial sites, has spectral parameters similar to the high-spin trigonal-planar ferrous complex (nacnac)FeMe reported by Holland and coworkers (δ = 0.48 mm/s, ΔE_Q = 1.74 mm/s).[27] The minor doublet (δ_2 = 0.92(4) mm/s, ΔE_Q = 1.18(4) mm/s) should thus correspond to the pseudotetrahedral environment on the equatorial sites, although the relative paucity of Mössbauer spectra available for such an environment required the synthesis of a model complex. Treatment of (tmeda)Fe($CH_2{}^tBu$)$_2$ with two equivalents of triphenylmethanol yields the high-spin ferrous alkoxide (tmeda)Fe($OCPh_3$)$_2$, which exhibits a Mössbauer spectrum (Figure 3, bottom) that is indeed consistent with the minor component in the spectrum of **[Fe_9O_6]** (δ = 0.97(2) mm/s, ΔE_Q = 1.12(2) mm/s). These data taken together support an all ferrous assignment.

The low coordination geometry and weak ligand fields in **[Fe_9O_6]** should lead to high-spin configurations for all ferrous ions, but the magnetic behavior of the cluster is not as easy to predict. Coupling between magnetic ions mediated by a diamagnetic bridge would generally favor antiferromagnetic coupling,[28,29] but the odd number of iron atoms would lead to a net magnetic moment.[30] Accordingly, Evans method measurements (Figure 4, left) reveal that solutions of **[Fe_9O_6]** at 298 K exhibit an effective magnetic moment that is *lower* than that expected for nine non-interacting high-spin Fe(II) centers (7.9 instead of 14.7), but considerably *higher* than expected for nine antiferromagnetically-coupled high-spin Fe(II) centers (net S = 2, expected μ_{eff} value ≅ 4.9).

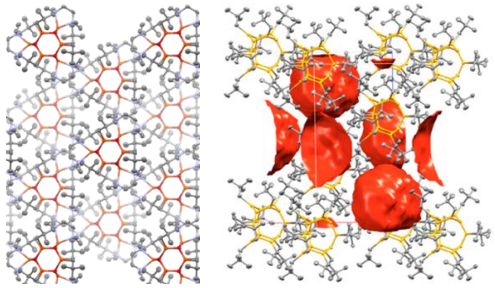

Figure 2. The solid-state packing of **[Fe_9O_6]** along the *c*-axis (right) highlight the axial alignment and three-fold symmetric packing of **[Fe_9O_6]** molecules. A depiction of the solid-state packing of **[Fe_9O_6]** highlighting the voids in the crystal lattice occupied by disordered solvent (left, or clarity, the Fe_9O_6 core is shown in yellow and the remaining ligands are shown in grey).

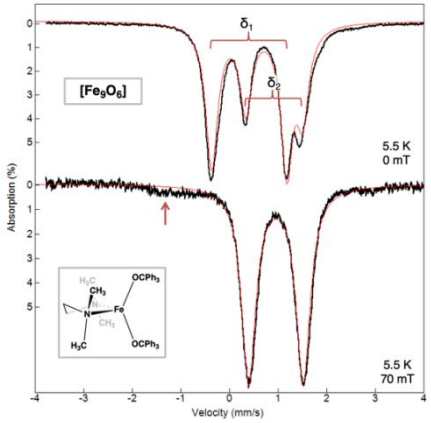

Figure 3. 5.5 K-Mössbauer spectra of crystalline **[Fe_9O_6]**•heptane (top, 0 T) and (tmeda)Fe($OCPh_3$)$_2$ (bottom, 70 mT). Data are shown in black hash-marks; the red lines are spectral fits with the parameters discussed in the text. Linewidths (FWHM) are 0.33 mm/s for **[Fe_9O_6]** and 0.30 mm/s for (tmeda)Fe($OCPh_3$)$_2$. The maroon arrow in the bottom panel indicates a broad, unidentified impurity accounting for less than 2 % of the total spectral area.

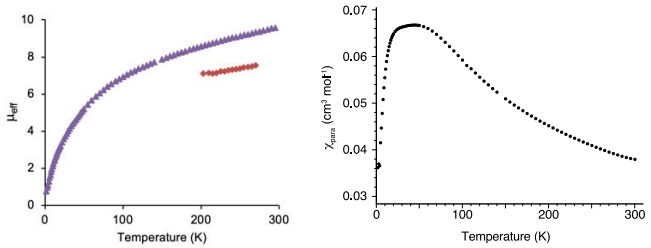

Figure 4. Left: Effective magnetic moment of **[Fe_9O_6]** in the solid state (SQUID, 1 T, purple) and in THF-d_8 solution (400 MHz ^{1}H NMR, maroon). Right: variable-temperature magnetometry of crystalline **[Fe_9O_6]**•heptane (SQUID, left) at 1T.

The solution-phase magnetic moment is weakly temperature dependent over the range from 200 K to 298 K, suggesting the complex has an S = 2 ground state with low-lying excited states that are thermally-accessible. Electronic structure calculations of a truncated model of the cluster ($Fe_9O_6(H)_6(NH_3)_6$) using the broken-symmetry formalism[31,32] are consistent with strong antiferromagnetic coupling leading to an S = 2 ground state (5 α Fe(II) + 4 β Fe(II)), with an energetically-accessible S = 6 excited state (6 α Fe(II) + 3 β Fe(II), +6.8 kcal/mol, expected μ_{eff} value = 13.0). The two electronic configurations differ in the relative spin orientation of one of the axial Fe atoms, wherein the first excited state has all the axial Fe environments antiferromagnetically coupled to the equatorial environments (Figure S4).

Magnetic susceptibility measurements performed on *solid* samples of **[Fe_9O_6]**•heptane reveal a higher effective magnetic moment value than found in solution (9.5 vs. 7.9 at 298 K). Upon decreasing the temperature, the effective magnetic moment value decreases monotonically, eventually reaching 0.8 at 2 K. This very low value implies that complexes are coupling with each other to lead to an overall singlet ground state for the compound. The temperature dependence of the molar magnetic susceptibility (χ_{para}) reveals Curie-Weiss behavior from 300 K to ~ 60 K (θ_P = –186 K at 1.0 T), whereupon the susceptibility levels out and then begins to decline below 20 K (Figure 4, right). The leveling-out behavior appears to be due to *two* discrete magnetic ordering events, occurring at 60 K and 20 K, which is unusual for molecular materials exhibiting simple antiferromagnetic coupling. Crystals of **[Fe_9O_6]** are axially symmetric (i.e. x = y ≠ z) (Figure 2) and interactions between clusters in the solid state may lead to complex magnetic behavior in polycrystalline samples, including multiple ordering events to relieve frustration. Using the higher ordering temperature (T_o) of 60 K, the degree of frustration (as $f = -\theta_P/T_o$)[33] of crystalline **[Fe_9O_6]**•heptane is calculated to be 3.10 at 1.0 T, indicating that this system is moderately frustrated. Magnetometry data could be fit using a four-parameter model, but the limited data results in an underdetermined mathematical system with several possible solutions (details in ESI); more detailed studies are underway.

Although the mechanism of formation of **[Fe_9O_6]** is difficult to elucidate, decades of research into the autoxidation of organometallic compounds, generally studied within the context of catalytic substrate oxidation, reveals that such reactions almost always favor free-radical chains.[34] Even noble metal organometallic systems, which usually terminate in alkoxide products from *formal* O-atom insertion into M-C bonds,[35–37] have been shown to proceed *via* radical steps initiated by binding of O_2 and formation of O-centered radicals. First row organometallics tend to yield O-atom insertion products,[38,39] and there is evidence that these proceed by way of the formation of metal dioxo intermediates.[40,41] The neopentanol and pivalaldehyde observed could be the result of rapid oxidation of neopentyl radicals produced upon coordination of O_2 to (tmeda)Fe($CH_2{}^tBu)_2$.[42–44] Oxidations under high concentrations of (tmeda)Fe($CH_2{}^tBu)_2$ seem essential, as the yield of **[Fe_9O_6]** was maximized *only* when the amount of residual (tmeda)Fe($CH_2{}^tBu)_2$ remained high (10 – 15%) – that is, reactions run to *complete* consumption of the dialkyl precursor actually resulted in *lower* yields of **[Fe_9O_6]** (< 5%). It is also notable that oxidation of (tmeda)Fe($CH_2{}^tBu)_2$ produces isolable amounts **[Fe_9O_6]** in either toluene or THF, but performing the same oxidation in pentane yields no isolable organometallic products. Given the weak C–H bonds in both toluene and THF, it seems plausible that these solvents are intercepting transient LFe^{III}-(O_2^-) species *via* formal H-atom transfer and minimizing the rate of aggregation and precipitation bulk iron oxide (Scheme 1).

Among the most notable aspects of this reaction is that since oxidation of Fe(II) precursors yields only Fe(II) oxide materials, it is conceivable that the iron-carbon bonds that are supplying the reducing equivalents. Low-coordinate organometallic complexes have considerable ionic character and have been used as formal sources of reduced metals,[45] and it seems possible that isolation of organometallic oxide clusters under substoichiometric oxidation conditions may be generalizable. Given the relatively low yield, the production of **[Fe_9O_6]** may be more a result of adventitious crystallization from a mixture of related clusters then the selective formation of just that core, but it is notable that the core bears the same Fe_nO_m stoichiometry as one of the 'magic-sized' clusters first observed by Sun *et al.* in gas phase experiments.[15,16] Such patterns are observed in noble metal and semiconductor cluster chemistry,[4,12] wherein part of the ability to isolate monodisperse clusters relies on magic numbers of elements that have a particular stability as monomers aggregate. Despite the presence of ligands and different oxidation state, the topology of the metal oxide core in **[Fe_9O_6]** is the same as predicted for the unligated cluster.

The self-assembly of a complex, reduced, low-coordinate organometallic cluster provides unique opportunities in synthetic chemistry. Gentle heating (65 ºC) of **[Fe_9O_6]** over the course of several hours in benzene, for example, results in the formation of dark precipitate and the formation of neopentane, suggesting **[Fe_9O_6]** is capable of C–H activation in a similar manner as related low-coordinate iron complexes.[46]

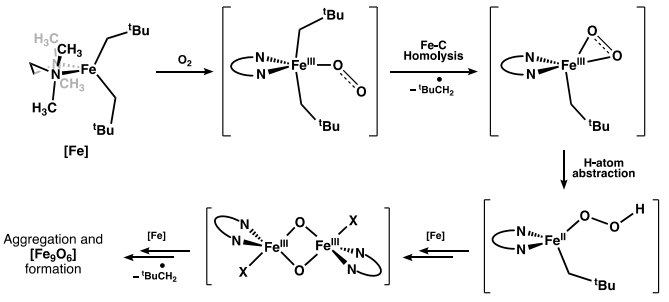

Scheme 1. One of the many possible oxidation cascade reactions leading to Fe-O bond formation during self-assembly of **[Fe_9O_6]**, where X indicates either neopentyl or alkoxide anionic ligands.

Acknowledgment

Generous support from the University of Wyoming Research Office, the UW Department of Chemistry, and the UW School of

Energy Resources is gratefully acknowledged. We also thank the UW Center for Photoconversion and Catalysis and NSF EPSCoR for undergraduate research fellowships (JAK). We would also like to thank Mr. Steve Adams and Mrs. Jane Adams of Cheyenne, WY for the generous donation of glassware. We gratefully acknowledge financial support from the National Science Foundation (CHE 0619920) and National Institute of General Medical Sciences of the National Institutes of Health (from the Institutional Development Award, Grant # 2P20GM103432). DFT calculations were performed on an allocation at the Advanced Research Computing Center at the University of Wyoming ("Teton", https://doi.org/10.15786/M2FY47). We are also indebted to Prof. Dean Roddick (UW) and Prof. Richard Finke (CSU) for helpful discussions. Dr. Popescu thanks the National Science Foundation Grant NSF-RUI 1445959, the University of St. Thomas (MN) and The College of Arts and Sciences for their generous support. BNL and MPS thank the NSF (CHE-1363274 and CHE-1800554) for support of solid-state magnetic studies.

Conflicts of interest

There are no conflicts to declare.

Notes and references

1 1 A. W. Castleman and P. Jena, *Proc. Natl. Acad. Sci.*, 2006, **103**, 10554–10559.
2 2 X.-K. Wan, S.-F. Yuan, Q. Tang, D. Jiang and Q.-M. Wang, *Angew. Chemie Int. Ed.*, 2015, **54**, 5977–5980.
3 3 R. Jin, *Nanotechnol. Rev.*, 2012, **1**, 31–56.
4 4 B. M. Cossairt, *Chem. Mater.*, 2016, **28**, 7181–7189.
5 5 M. R. Friedfeld, J. L. Stein and B. M. Cossairt, *Inorg. Chem.*, 2017, **56**, 8689–8697.
6 6 A. N. Beecher, X. Yang, J. H. Palmer, A. L. Lagrassa, P. Juhas, S. J. L. Billinge and J. S. Owen, *J. Am. Chem. Soc.*, 2014, **136**, 10645–10653.
7 7 J. Owen and L. Brus, *J. Am. Chem. Soc.*, 2017, **139**, 10939–10943.
8 8 C. Goh, B. M. Segal, J. Huang, J. R. Long and R. H. Holm, *J. Am. Chem. Soc.*, 1996, **118**, 11844–11853.
9 9 X. Roy, C.-H. Lee, A. C. Crowther, C. L. Schenck, T. Besara, R. A. Lalancette, T. Siegrist, P. W. Stephens, L. E. Brus, P. Kim, M. L. Steigerwald and C. Nuckolls, *Science (80-.).*, 2013, **341**, 157–160.
10 10 R. Hernández Sánchez and T. A. Betley, *J. Am. Chem. Soc.*, 2015, **137**, 13949–13956.
11 11 R. Hernández Sánchez, A. K. Bartholomew, T. M. Powers, G. Ménard and T. A. Betley, *J. Am. Chem. Soc.*, 2016, **138**, 2235–2243.
12 12 D. C. Gary, S. E. Flowers, W. Kaminsky, A. Petrone, X. Li and B. M. Cossairt, *J. Am. Chem. Soc.*, 2016, **138**, 1510–1513.
13 13 M. Bosch, S. Yuan, W. Rutledge and H.-C. Zhou, *Acc. Chem. Res.*, 2017, **50**, 857–865.
14 14 A. Fernando, K. L. D. M. Weerawardene, N. V. Karimova and C. M. Aikens, *Chem. Rev.*, 2015, **115**, 6112–6216.
15 15 Q. Wang, Q. Sun, M. Sakurai, J. Z. Yu, B. L. Gu, K. Sumiyama and Y. Kawazoe, *Phys. Rev. B*, 1999, **59**, 12672–12677.
16 16 Q. Sun, M. Sakurai, Q. Wang, J. Z. Yu, G. H. Wang, K. Sumiyama and Y. Kawazoe, *Phys. Rev. B*, 2000, **62**, 8500–8507.
17 17 S. Yin, W. Xue, X.-L. Ding, W.-G. Wang, S.-G. He and M.-F. Ge, *Int. J. Mass Spectrom.*, 2009, **281**, 72–78.
18 18 F. Bottomley and F. Grein, *Inorg. Chem.*, 1982, **21**, 4170–4178.
19 19 G. de Ruiter, N. B. Thompson, D. Lionetti and T. Agapie, *J. Am. Chem. Soc.*, 2015, **137**, 14094–14106.
20 20 S. M. Gorun and S. J. Lippard, *Nature*, 1986, **319**, 666–668.
21 21 A. L. Barra, F. Bencini, A. Caneschi, D. Gatteschi, C. Paulsen, C. Sangregorio, R. Sessoli and L. Sorace, *Chemphyschem*, 2001, **2**, 523+.
22 22 S. G. Baca, M. Speldrich, J. Van Leusen, A. Ellern and P. Kögerler, *Dalt. Trans.*, 2015, **44**, 7777–7780.
23 23 A. A. Kitos, C. Papatriantafyllopoulou, A. J. Tasiopoulos, S. P. Perlepes, A. Escuer and V. Nastopoulos, *Dalt. Trans.*, 2017, 3240–3251.
24 24 L. Yang, D. R. Powell and R. P. Houser, *Dalt. Trans.*, 2007, 955–964.
25 25 L. Noodleman, C. Y. Peng, D. A. Case and J.-M. Mouesca, *Coord. Chem. Rev.*, 1995, **144**, 199–244.
26 26 H. Beinert, R. H. Holm and E. Münck, *Science (80-.).*, 1997, **277**, 653–659.
27 27 H. Andres, E. L. Bominaar, J. M. Smith, N. A. Eckert, P. L. Holland and E. Münck, *J. Am. Chem. Soc.*, 2002, **124**, 3012–3025.
28 28 J. Kanamori, *J. Phys. Chem. Solids*, 1959, **10**, 87–98.
29 29 J. B. Goodenough, *Chem. Mater.*, 2014, **26**, 820–829.
30 30 C. Lacroix, P. Mendels and F. Mila, Eds., *Introduction to Frustrated Magnetism*, Springer Berlin Heidelberg, Berlin, Heidelberg, 2011, vol. 164.
31 31 L. Noodleman, *J. Chem. Phys.*, 1981, **74**, 5737–5743.
32 32 E. Ruiz, in *Comprehensive Inorganic Chemistry II*, Elsevier, 2013, vol. 9, pp. 501–549.
33 33 A. P. Ramirez, *Annu. Rev. Mater. Sci.*, 1994, **24**, 453–480.
34 34 L. Boisvert and K. I. Goldberg, *Acc. Chem. Res.*, 2012, **45**, 899–910.
35 35 V. V Rostovtsev, J. A. Labinger, J. E. Bercaw, T. L. Lasseter and K. I. Goldberg, *Organometallics*, 1998, **17**, 4530–4531.
36 36 J. D. Prantner, W. Kaminsky and K. I. Goldberg, *Organometallics*, 2014, **33**, 3227–3230.
37 37 B. V. Popp and S. S. Stahl, *J. Am. Chem. Soc.*, 2007, **129**, 4410–4422.
38 38 C. Ni and P. P. Power, *Chem. Commun.*, 2009, 5543.
39 39 P. Zhao, H. Lei, C. Ni, J.-D. Guo, S. Kamali, J. C. Fettinger, F. Grandjean, G. J. Long, S. Nagase and P. P. Power, *Inorg. Chem.*, 2015, **54**, 8914–8922.
40 40 B. M. Prince, T. R. Cundari and C. J. Tymczak, *J. Phys. Chem. A*, 2014, **118**, 11056–11061.
41 41 F. Dai, G. P. A. Yap and K. H. Theopold, *J. Am. Chem. Soc.*, 2013, **135**, 16774–16776.
42 42 I. Fernández, R. J. Trovitch, E. Lobkovsky and P. J. Chirik, *Organometallics*, 2008, **27**, 109–118.
43 43 D. Wu and K. D. Bayes, *Int. J. Chem. Kinet.*, 1986, **18**, 547–554.
44 44 H. Sun and J. W. Bozzelli, *J. Phys. Chem. A*, 2004, **108**, 1694–1711.
45 45 J. F. Ackerman, *Mater. Res. Bull.*, 1988, **23**, 165–169.
46 46 K. C. MacLeod, R. A. Lewis, D. E. DeRosha, B. Q. Mercado and P. L. Holland, *Angew. Chemie Int. Ed.*, 2017, **56**, 1069–1072.

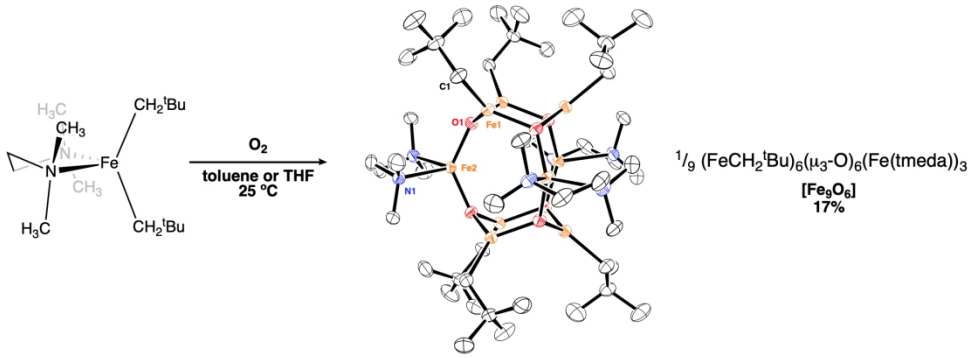
H3C
CH3
N
Fe
CH3
H3C
CH2tBu
CH2tBu
O2
toluene or THF
25 °C
C1
O1
Fe1
Fe2
N1
1/9 (FeCH2tBu)6(μ3-O)6(Fe(tmeda))3
[Fe9O6]
17%